Tight junction protein claudin-2 promotes self-renewal of human colorectal cancer stem-like cells

Sophie Paquet-Fifield[a], Shir Lin Koh[a], Lesley Cheng[b], Laura M. Beyit[a], Carolyn Shembrey[a], Christina Mølck[a], Corina Behrenbruch[a,c], Marina Papin[d,e,f], Meritxell Gironella[g], Sophie Guelfi[d,e,f], Ramona Nasr[d,e,f], Fanny Grillet[d,e,f] Michel Prudhomme[h], Jean-Francois Bourgaux[i], Antoni Castells[g], Jean-Marc Pascussi[d,e,f], Alexander G. Heriot[c], Alain Puisieux[j], Melissa J. Davis[k], Julie Pannequin[d,e,f], Andrew F. Hill[b], Erica Sloan[c, l, m], Frédéric Hollande[a #]

[a] Department of Pathology, The University of Melbourne, Victorian Comprehensive Cancer Centre, Parkville, VIC3010, Australia
[b] Department of Biochemistry and Genetics, La Trobe Institute for Molecular Science, La Trobe University, Australia
[c] Peter MacCallum Cancer Centre, Division of Cancer Surgery, Victorian Comprehensive Cancer Centre, Parkville, VIC 3010, Australia.
[d] Centre National de la Recherche Scientifique (CNRS), UMR5203, Institut de Génomique Fonctionnelle, Montpellier, F-34094 France
[e] Institut National de la Santé et de la Recherche Médicale (INSERM), U661, Montpellier, France
[f] Université Montpellier 1 et 2, UMR5203, Montpellier, France
[g] Gastrointestinal and Pancreatic Oncology Group, Hospital Clínic of Barcelona, Centro de Investigación Biomédica en Red de Enfermedades Hepáticas y Digestivas (CIBEREHD), Institut d'Investigacions Biomèdiques August Pi i Sunyer (IDIBAPS), Barcelona, Spain.
[h] Department of Surgery, Hopital Carémeau, F-30000 Nimes
[i] Department of Gastroenterology, Hopital Carémeau, F-30000 Nimes
[j] Cancer Research Center of Lyon, Lyon, F-69008, France
[k] Bioinformatics Division, The Walter and Eliza Hall Institute of Medical Research, Parkville, VIC, 3052, Australia.
[l] Monash Institute of Pharmaceutical Sciences, Drug Discovery Biology Theme, Monash University, Parkville VIC 3052, Australia
[m] Cousins Center for PNI, UCLA Semel Institute, Jonsson Comprehensive Cancer Center, and UCLA AIDS Institute, University of California Los Angeles, Los Angeles, CA 90095, USA.

Corresponding author: A/Prof Frédéric Hollande, Department of Pathology, The University of Melbourne, Level 10, Victorian Comprehensive Cancer Centre, Grattan Street, Parkville VIC 3010, Australia. Ph: +613 8559 7023; email: frederic.hollande@unimelb.edu.au

Disclosure of Potential Conflicts of Interest: The authors declare no potential conflicts of interest.

Running title: Claudin-2 promotes self-renewal of human CRC stem-like cells

Keywords: cancer stem cells, intra-tumor heterogeneity, plasticity, self-renewal, miRNA, YAP

Grant support: This work was supported by the National Health and Medical Research Council (NHMRC) of Australia (#1049561, #1069024) and the French Association pour la Recherche contre le Cancer (ARC)(#5046).

Statement of significance: The Tight Junction protein claudin-2 promotes the self-renewal of colorectal cancer stem cells through the regulation of YAP activity and miR-222-3p expression

Word count: 5,115 words; **Total number of figures:** 7

Abstract

Post-treatment recurrence of colorectal cancer (CRC), the third most lethal cancer worldwide, is often driven by a subpopulation of cancer stem cells (CSCs). The tight junction (TJ) protein claudin-2 is overexpressed in human CRC where it enhances cell proliferation, colony formation, and chemoresistance *in vitro*. While several of these biological processes are features of the CSC phenotype, a role for claudin-2 in the regulation of these has not been identified. Here we report that elevated claudin-2 expression in stage II/III colorectal tumors is associated with poor recurrence-free survival following 5-FU-based chemotherapy, an outcome in which CSC play an instrumental role. In patient-derived organoids, primary cells, and cell lines, claudin-2 promoted CRC self-renewal in vitro and in multiple mouse xenograft models. Claudin-2 enhanced self-renewal of $ALDH^{High}$ CSC and increased their proportion in CRC cell populations, limiting their differentiation and promoting the phenotypic transition of non-CSC towards the $ALDH^{High}$ phenotype. Next-generation sequencing in $ALDH^{High}$ cells revealed that claudin-2 regulated expression of nine microRNAs known to control stem cell signaling. Among these, miR-222-3p was instrumental for the regulation of self-renewal by claudin-2, and enhancement of this self-renewal required activation of YAP, most likely upstream from miR-222-3p. Taken together, our results indicate that overexpression of claudin-2 promotes self-renewal within CRC stem-like cells, suggesting a potential role for this protein as a therapeutic target in CRC.

Introduction

Claudins are transmembrane proteins involved in tight junction (TJ) formation and function within healthy epithelia, endothelia, and other tissues (1). Claudins have been implicated in multiple biological processes, including the regulation of paracellular transport of solutes and water, the maintenance of epithelial tissue integrity, the maintenance of apico-basal polarity and the specification of morphology in embryos and tissues (2). Their expression is altered in several cancer types, and a tumor-promoting role has been suggested for several claudin isoforms (3), including in colorectal cancer (CRC) (4,5). In particular, claudin-2 is overexpressed in a significant proportion of human colorectal tumors (6,7), and we recently demonstrated that this protein is instrumental to the tumor-promoting activity of the transcriptional regulator symplekin in CRC cells (8). Claudin-2 also promotes proliferation and anchorage-independent colony formation by human CRC cells *in vitro*, and increases tumor growth in xenografted mice (6).

Claudin-2 expression is restricted to the stem/progenitor cell compartment in the healthy intestinal epithelium (9), and its regulatory role in intestinal homeostasis was recently highlighted (10). We also detected enriched claudin-2 expression in mouse intestinal tumors displaying elevated expression of cancer stem cell (CSC) markers and Wnt target genes (11). Additionally, claudin-2 was recently shown to promote anchorage-independent growth and to enhance resistance to 5-FU (6). While several of these properties are among those that characterize CSCs (12), a putative role for claudin-2 in the regulation of these cells remains to be explored.

Since many colorectal tumors overexpress claudin-2 we tested the hypothesis that high claudin-2 expression may contribute to the regulation of stem-like cells within these tumors. We found that claudin-2 overexpression was associated with reduced post-chemotherapy disease-free survival in three independent cohorts of CRC patients, and that claudin-2-overexpressing cells displayed elevated self-renewal *in vitro* and tumor-initiation frequency *in vivo*. Claudin-2 increased the proportion of $ALDH^{High}$ cancer stem-like cells in heterogeneous CRC cell populations, and this outcome was due to enhanced $ALDH^{High}$ cell self-renewal and to a higher conversion rate of $ALDH^{Low}$ into $ALDH^{High}$ cells. Claudin-2 selectively regulated the expression of 9 miRNAs in $ALDH^{High}$ cells, and miR-222-3p regulation was instrumental for the promotion of self-renewal by claudin-2. Finally, activation of YAP by claudin-2, most likely upstream from miR-222-3p was also essential to this effect. Our results indicate that elevated expression of claudin-2 promotes self-renewal within CRC stem-like cells, suggesting a potential role for this protein as a prognostic marker and/or a therapeutic target in CRC.

Materials and Methods

Further details concerning constructs/reagents, cell lines and patient-derived tumor cells culture, CLDN2 expression/survival associations, in-vivo experiments, RNA extraction, real-time PCR, Western blotting, ALDH activity-based cell sorting, immunohistochemistry, sphere formation assays and miRNA quantification and rescue experiments are provided in Supplemental Methods and Supplemental Table S1.

Association between CLDN2 expression and CRC patient survival

The association between CLDN2 mRNA expression and disease outcome in patients with stage II/III CRC treated with 5-FU-based chemotherapy was analyzed in three independent datasets. Quantification of CLDN2 mRNAs from paraffin-embedded sections using RT-qPCR and correlation with patient survival was performed on a cohort treated at the Hospital Clínic of Barcelona in 1998-2005 (13)(14). Two other datasets were selected based on the presence of CLDN2-specific probes, the number of patients (>150), and the availability of recurrence-free survival data. GSE24551- GPL11028 (15), was sourced and analyzed using the SurvExpress bioresource, (http://bioinformatica.mty.itesm.mx:8080/Biomatec/SurvivaX.jsp)(16). GSE39582 (17)(461 patients) was analyzed using the R2: Genomics Analysis and Visualization Platform (http://r2.amc.nl).

Patient-derived samples

All experiments including patient samples were performed in accordance with ethical principles for medical research involving human subjects as set by the Declaration of Helsinki. Patient-derived colon cancer cells (CPP) were derived detailed under Supplemental Methods from CRC biopsies obtained from Centre Hospitalier Universitaire (CHU) Carémeau (Nimes, France). The protocol was approved by the CHU Institutional Ethics Committee (Human ethics agreement #2011-A01141-40, NCT01577511). Patient-derive organoids were grown from samples collected under human ethic agreement HREC/15/PMCC/112, Peter MacCallum Cancer Centre Human Research Ethics Committee, Melbourne, Australia. Signed informed consents were obtained from all patients prior to samples acquisition.

miRNA quantification

RNA including miRNAs were isolated using the miRNeasy mini kit (QIAGEN) and RNA quality was analyzed on the Agilent 2100 Bioanalyzer™. Deep sequencing was run on an Ion Torrent PGM™sequencer, using Ion™ 318 V2 chips and Ion PGM™ 200 V2 Sequencing Kit (Life Technologies). Sequence files were analyzed for quality control (FASTQC), aligned to the Human genome (HG19) using the Torrent Suite and transferred to Partek Genomic Suite and Flow (Partek Incorporated, Singapore) for mapping against miRBase V.21 and Ensembl Release 75. Reads were normalized to reads per million reads and miRNAs identified with at least 10 reads were used for further analysis on Partek Genomic suite.

Cell lines

Cell lines used in the present study were obtained from the American Tissue Culture Collection (ATCC). Experiments were performed within a maximum of 10 passages after thawing, and the absence of

mycoplasma was confirmed monthly using the MycoAlert™ Mycoplasma Detection Kit (Lonza). All cell lines were authenticated using STR profiling (LGC standards).

In vivo experiments

Several xenograft models were used under agreements from the Monash Institute of Pharmaceutical Sciences Animal Ethics Committee (#MIPS_AEC2012.04 and #MIPS_AEC2013.01) to analyze the impact of claudin-2 on self-renewal.

To analyze the role of claudin-2 on primary tumor initiation, tumor incidence was monitored after subcutaneous injection of CPP1 or CMT93 cells to NOD/SCID mice. For serial transplantation, first generation tumors were collected when reaching 500 mm^3 and dissociated using the gentleMACS dissociator (Miltenyi Biotec). Viable (DAPI-negative) cells were serially transplanted into the flank of new NOD/SCID mice.

To assess the role of claudin-2 on metastasis initiation, luciferase-expressing CPP1 cells were injected into the caecum of NOD/SCID mice. Primary tumor growth and metastasis development were monitored for 6 weeks using Bio-Luminescence Imaging (BLI). 47 days after injection animals were euthanized and their liver was imaged *ex-vivo*.

To characterize the impact of claudin-2 on post-chemotherapy tumor recurrence, NOD/SCID mice were injected subcutaneously with T84 cells. When tumors reached 250 +/- 25 mm^3, mice were treated with FOLFIRI (40mg/kg 5-fluorouracil + 15mg/kg Irinotecan + 30mg/kg Leucovorin, 2x/week, 3 weeks). Post-treatment residual tumors were dissociated and tumor cells re-implanted into second generation animals.

Statistical analysis

Graphpad Prism6 software was used for data analysis. After determining whether or not datasets for each experiment were normally distributed, a Student's t-test or a Mann and Whitney test was performed to analyze the difference between two groups of quantitative variables, as indicated in the figure legends. ANOVA was used for comparisons among three groups of quantitative variables, and pairwise comparisons were carried out using the Tukey post-hoc test as indicated. Statistical significance of stem cell frequencies quantified using Extreme Limiting Dilution Analysis (ELDA) was assessed using the Chi-Square test, as described previously (18).

Results

Elevated CLDN2 expression in human CRC is linked with post-treatment recurrence.

CSCs play a key role in the poor clinical outcome of CRC patients treated with adjuvant chemotherapy (19,20). To determine whether claudin-2 overexpression may contribute to these outcomes, we first

quantified prospectively the expression of *CLDN2* mRNA in a homogenous population of primary tumor samples from patients with stage II/III CRC that were all treated with 5-FU-based adjuvant chemotherapy (14). *CLDN2* mRNA was detected in 86 patient samples using RT-qPCR, and Kaplan-Meier analysis showed that high *CLDN2* expression correlated with lower cancer specific survival (p=0.0329) (Figure 1A).

We also performed a retrospective analysis of published datasets to determine whether *CLDN2* mRNA expression level in primary colorectal tumors would be associated with specific disease outcomes. We used a large cohort of CRC patients from the GSE39582 dataset (17), from which patients with stage II/III tumors, who are usually administered adjuvant chemotherapy, were selected using the R2 Genomics Analysis and Visualization Platform (Figure 1B). High *CLDN2* expression levels correlated with poorer probability of relapse-free survival in these patients (p=0.049, n=461). A stage-specific analysis showed the same trend for stage II (p=0.058, n=260) and stage III (p=0.053, n=201) (Supplemental Figure S1). Finally, using another homogenous cohort of colon cancer patients with stage II/III CRC (GSE24551)(15), we found that patients with high *CLDN2* mRNA expression displayed significantly worse recurrence-free survival following adjuvant chemotherapy than those expressing low levels of claudin-2 (p=0.0094, n=160, Figure 1C-D).

To determine whether these changes were detectable at protein level, we performed claudin-2 immunostaining on a tissue microarray (TMA) containing primary tumor sections from 24 patients with stage II and III CRC having undergone 5-FU-based adjuvant chemotherapy (Supplemental Table S2). Despite the small size of this cohort, our results (Figure 1E and Supplemental Figure S1) highlighted the positive association trend between claudin-2 expression and the presence of post-treatment recurrence in these patients (chi-square=3.696, p=0.0545). No correlation was detected between the cellular localization of claudin-2 staining (categorized into membrane, cytoplasmic/nuclear, or mixed pattern staining) and post-treatment recurrence (chi-square=1.252, p=0.2631, Supplemental Figure S1).

These results demonstrate that increased *CLDN2* expression within stage II/III colorectal tumors is associated with poor recurrence-free survival in patients treated with adjuvant chemotherapy.

Claudin-2 promotes the self-renewal of CRCs *in vitro*.

CSCs have frequently been identified as important drivers of post-chemotherapy recurrence (12,21). Using CRC cells isolated from colon tumor biopsies and established CRC cell lines, we therefore analyzed the impact of claudin-2 overexpression on self-renewal, a core functional characteristic of CSCs.

We first induced claudin-2 overexpression in a CRC cell line (SW480) expressing low levels of endogenous claudin-2, as shown in Figure 2A. Claudin-2 overexpression strongly enhanced the ability of these cells to form colonospheres over multiple passages in suspension (Figure 2B), an *in vitro* hallmark of self-renewing cells (22). The size of claudin-2-overexpressing colonospheres was enlarged compared to those of controls and claudin-2-overexpressing colonospheres survived for more than 1 month without passaging, in contrast with the rare spheres formed by control cells (Supplemental Figure S2). We also

analyzed the impact of claudin-2 overexpression on long-term self-renewal in patient-derived cells generated from a primary colon cancer sample (CPP1), using serial passaging followed by an ELDA assay. Claudin-2 expression increased the stem cell frequency of 10^{th} generation cells from 1 in every 23.4 cells (confidence interval 1/11.5 - 1/47.4) to 1 in every 7 (1/3.7 - 1/13.4) (Figure 2C). Goodness of fit analysis highlighted the significant difference between control and claudin-2-expressing cells (Pearson Chi-square = 5.25, p=0.0219).

Conversely, we used several approaches to down-regulate claudin-2 expression in CRC cells expressing high endogenous levels of this protein. Inducible shRNA-mediated claudin-2 down-regulation in DLD-1 cells significantly decreased their colonosphere-forming ability (Figure 2D) and hampered colonosphere growth compared to controls (Supplemental Figure S2). Similar results were obtained in T84 CRC cells (Figure 2E) using shRNAs targeting a different region of the *CLDN2* gene. Claudin-2 down-regulation or overexpression did not alter the expression of claudin-1 (Supplemental Figure S2), another claudin isoform previously shown to play a regulatory role in CRC (5), highlighting the claudin-2 specificity of this effect. To further corroborate whether claudin-2 expression regulates CSC-driven biological processes in primary cells, CLDN2-selective siRNAs were transfected into tumor organoids grown from surgically resected primary colorectal tumors. The initiation of CRC organoids was significantly decreased from three days after transfection with siCLDN2 (Mean organoid number ± S.E.M = 19.64 ± 2.37) in comparison with siCON-transfected organoids (Mean ± S.E.M = 34.62 ± 5.30) (p = 0.0426, ANOVA with Tukey's test) (Figure 2F), suggesting that claudin-2 expression regulates organoid initiation in primary CRC cells.

Together these findings indicate that claudin-2 promotes self-renewal of colon cancer cells *in vitro*, a key characteristic of CSCs.

Claudin-2 promotes CRC self-renewal *in vivo*.

An important feature of CSCs is their capacity to initiate tumors when injected at low concentration into immunocompromised animals (23). To determine whether claudin-2 regulates CSC self-renewal *in vivo*, patient-derived CPP1 cells were transfected to stably overexpress claudin-2 (Supplemental Figure S3), and increasing numbers of these cells (50, 500 and 5000) were subcutaneously grafted into immune compromised NOD/SCID mice. Tumor initiation was readily detected in mice inoculated with claudin-2-overexpressing cells, with 3/5 mice injected with as little as 50 cells bearing detectable tumors by day 90 after injection (Figure 3A). In contrast, no tumors were detected by day 90 following the injection of 50 control CPP1 cells. Tumor initiation was strongly delayed in mice injected with 500 or 5000 control cells compared to claudin-2-expressing CPP1 (Figure 3A), and tumor growth was reduced (Supplemental Figure S3).

To determine whether the claudin-2-driven self-renewal increase was maintained after passaging, cells from claudin-2-overexpressing xenografts (500 cell group) were dissociated once tumors reached a $500mm^3$ volume, and re-implanted subcutaneously into new mice. Tumor initiation was detected in second-

generation animals injected with 50 (1/5), 500 (4/5) and 5000 (4/5) claudin-2-overexpressing cells (Figure 3A), but serial transplantation of tumor cells was not successful from control tumor cells, as insufficient live cells could be recovered from the small control tumors (< 35 mm^3).

To determine whether the promotion of tumor initiation by claudin-2 extends beyond human CRC cells, we overexpressed claudin-2 in CMT93 mouse rectal carcinoma cells (Supplemental Figure S3) and injected them into NOD/SCID mice (10, 100, or 100 cells/mouse) to determine their maximal engraftment efficiency (Figure 3B). 37 days after injection, tumors had developed in mice from all claudin-2 overexpressing groups, including 20% (1/5) of mice inoculated with 10 cells (Figure 3B). In contrast, tumors were only detectable in 4/5 mice inoculated with 1000 control cells but not in those injected with 10 or 100 control cells. (Figure 3B and Supplemental Figure S3). Tumors were collected and claudin-2 immunostaining was used to validate claudin-2 overexpression in this tumor model (Figure 3B).

To examine whether the metastasis-initiating ability of CRC cells is regulated by claudin-2, we performed intra-caecal injection of luciferase-expressing CPP1 cells (1×10^5/mouse) and monitored liver metastasis development for 6 weeks using bio-luminescent imaging. All mice developed primary tumors, and 2/3 mice injected with claudin-2-overexpressing CPP1 cells also developed liver metastases, while none of the 5 control mice did (Supplemental Figure S4). 2/5 mice injected with claudin-2-overexpressing cells spontaneously died 2-3 weeks after injection and had to be excluded from the analysis.

Finally, to characterize the impact of claudin-2 on the recurrence potential of CRC cells after chemotherapy, NOD/SCID mice were injected subcutaneously with T84 cells expressing a control or a claudin-2-specific shRNA (n=18/group, 1 x 10^6 cells/mouse). When tumors reached 250 +/- 25 mm^3, mice were treated for 3 weeks with FOLFIRI. Residual tumors were dissociated and live tumor cells re-implanted subcutaneously into second generation animals (50, 500, 5000 cells/mouse, 6 mice/group). 8 weeks later, cells expressing claudin-2 shRNA displayed reduced ability to initiate second-generation tumors at all concentrations compared to control cells (Figure 3C).

Together these findings demonstrate that claudin-2 promotes the primary and metastatic tumor-initiating capacity of CRC cells as well as their self-renewing ability after exposure to chemotherapy *in vivo*, which are both recognized properties of CSCs.

Claudin-2 regulates phenotypic transitions between CSC and non-CSC states *in vitro.*

We demonstrated above that claudin-2 overexpression enhances tumor initiation *in vivo* and CRC cell self-renewal *in vitro*, suggesting that this protein may increase the proportion and/or self-renewal potential of stem-like cells in colon cancer. To gain further mechanistic insight we first investigated whether claudin-2 had an impact on the expression of stem cell markers such as *BMI1*, *POU5F1* (Oct-4), and *ALDH1A1*. Levels of mRNA encoding BMI1, ALDHA1, and Oct-4 were significantly decreased in T84 cells where claudin-2 expression was constitutively down-regulated (CLDN2-shRNA cells, Figure 4A). Short-term

claudin-2 down-regulation using siRNA decreased the expression of some but not all of these markers in DLD-1, T84, and patient-derived CPP42 cells, suggesting that sustained claudin-2 down-regulation may be required to transcriptionally regulate stem cell markers (Figure 4B).

Since elevated enzymatic activity of aldehyde dehydrogenase has been reported as a robust marker to enrich CSCs (24), we examined whether claudin-2 expression differed in flow cytometry-enriched $ALDH^{High}$ versus $ALDH^{Low}$ cells. *CLDN2* mRNA levels were 2.3-fold higher in $ALDH^{High}$ than in $ALDH^{Low}$ T84 cells (6.96±0.15 *vs* 2.84±0.73 respectively) (Figure 4C). To determine whether claudin-2 expression impacts on the proportion of $ALDH^{High}$ cells within heterogeneous cancer cell populations, we transfected T84 cells with CLDN2-selective or with control siRNA. Three days later, control siRNA did not alter homeostatic proportions of $ALDH^{High}$ and $ALDH^{Low}$ cells (33 ± 4% and 66 ± 5.2%, respectively) compared to un-transfected cells (35 ± 5% and 65 ± 5%) (Figure 4D). In contrast, claudin-2 down-regulation significantly reduced the proportion of $ALDH^{High}$ cells (17 ± 2% $ALDH^{High}$ and 83 ± 6.5% $ALDH^{Low}$ cells) (Figure 4D).

Because the rate of phenotypic transitions between stem-like and non-stem cells was shown to modulate homeostatic proportions between these phenotypes in breast cancer (25), we analyzed whether claudin-2 could alter phenotypic transitions between $ALDH^{High}$ and $ALDH^{Low}$ cells in CRC cells. $ALDH^{High}$ and $ALDH^{Low}$ subpopulations were purified from T84 cells using flow cytometry, transfected independently with CLDN2-selective or control siRNA, and seeded as adherent layers in complete medium. Efficiency of claudin-2 down-regulation was similar in $ALDH^{High}$ (86% inhibition compared to controls) and $ALDH^{Low}$ cells (79% inhibition). Claudin-2 down-regulation was transient, with maximal reduction attained by 24h, followed by a progressive return to control levels (days 3-6) (Supplemental Figure S5).

The percentage of $ALDH^{High}$ and $ALDH^{Low}$ populations was then quantified 3 and 6 days after transfection to determine what proportion of the pure $ALDH^{high}$ or $ALDH^{low}$ subpopulations seeded were able to convert to a different ALDH phenotype (Figure 4E).

Transition from $ALDH^{High}$ towards $ALDH^{Low}$ phenotype was a rapid process. In controls 58% ± 5% $ALDH^{Low}$ cells were detected by day 3 after seeding purified $ALDH^{High}$ populations. This transition was faster in cells transfected with claudin-2 siRNA, where 72 ± 5.9% $ALDH^{low}$ cells were detected by day 3. After 6 days, claudin-2 mRNA expression was back to control levels (Supplemental Figure S5) and proportions of $ALDH^{High}$ and $ALDH^{Low}$ populations were no longer different in cells that had been transfected with control (28% $ALDH^{High}$ and 72% $ALDH^{Low}$) or with claudin-2 siRNA (34% $ALDH^{High}$ and 66% $ALDH^{Low}$) (Figure 4E). This result indicates that the transient down-regulation of claudin-2 was responsible for enhancing the phenotypic transition from $ALDH^{High}$ to $ALDH^{Low}$ cells.

Conversely, we analyzed whether the transitions from $ALDH^{Low}$ to $ALDH^{High}$ was also controlled by claudin-2. Purified $ALDH^{Low}$ cells were able to reconstitute an $ALDH^{High}$ population, albeit at a slower rate than the $ALDH^{High}$ to $ALDH^{Low}$ conversion (Figure 4D). $ALDH^{Low}$ cells transfected with control siRNA generated 15 ± 1.9% $ALDH^{High}$ cells by 3 days and 25 ± 10.2% by 6 days after transfection. Claudin-2

down-regulation in ALDH^{Low} cells reduced the rate of conversion into ALDH^{High} cells, with only 2.5 ± 0.3% newly formed ALDH^{High} cells at day 3. The proportion of ALDH^{Low} cells converting to an ALDH^{High} phenotype increased to 13 ± 3.4% by day 6, when the claudin-2 siRNA is no longer effective. Similar results were obtained with the DLD-1 cell line (Supplemental Figure S6).

Taken together this data demonstrate that claudin-2 enhances proportions of ALDH^{High} stem-like cells by stabilizing the ALDH^{High} cell phenotype and favoring phenotypic transitions from ALDH^{Low} towards ALDH^{High} subpopulations.

Claudin-2 regulates the self-renewal capacity of ALDH^{High} cells.

We demonstrated above that claudin-2 regulates homeostatic proportions of ALDH^{High} cells within heterogeneous colon cancer cell populations. To establish whether this is reflected by an increased self-renewal frequency of ALDH^{High} cells, we FACS-purified ALDH^{High} T84 cells and transfected them in suspension with claudin-2-selective or control siRNA. 12 hours later these cells were seeded in an ELDA assay and the stem cell frequency of each cell population was quantified after 10 days as previously described (18). Claudin-2 down-regulation significantly decreased the stem cell frequency from 1 in every 6.24 cells (confidence interval 1/3.31 - 1/11.8) to 1 in every 39.8 cells (1/21.2 - 1/74.8) (Chi-square test ($\chi 2$= 14.6, * p=0.000132) (Figure 5A).

To determine whether claudin-2 alters the tumor-initiating potential of ALDH^{High} cells *in vivo*, purified ALDH^{High} T84 cells were transiently transfected as described above and grown overnight to ensure optimal *CLDN2* down-regulation. Since our results (Figure 4) indicated that phenotypic transitions from ALDH^{High} to ALDH^{Low} population occurs rapidly, transfected ALDH^{High} cells were re-purified by FACS prior to subcutaneous injection into SCID/NOD mice (500 cells/injection) to minimize the dilution of the ALDH^{High} population. Six weeks after injection, 5/5 mice inoculated with siCON-transfected ALDH^{High} cells generated tumors while 2/5 mouse only exhibited a measurable tumor following inoculation of ALDH^{High} expressing claudin-2 siRNA (Figure 5B-C). These findings demonstrate that claudin-2 down-regulation in T84 ALDH^{High} CSC-like cells impairs their ability to initiate tumors *in viv*o.

We also quantified the endogenous claudin-2 expression levels and the stem cell frequency in 10 different patient-derived cell lines, and found that cell populations containing low proportions of self-renewing cells (< 2 % of the total population, n= 5 patient-derived cell populations) expressed lower levels of claudin-2 mRNA (average 1/dCp = 0.060 +/- 0.0006, n=5) compared to those displaying higher proportions (1/dCp = 0.089 +/- 0.009, n=5) (Figure 5D). These data suggest that elevated claudin-2 expression is linked with a high self-renewal frequency in CRC cells.

Overall, our findings demonstrate that claudin-2 directly modulates the self-renewal and tumor-initiating ability of ALDH^{High} colorectal CSCs.

Claudin-2 regulates the expression miR-222-3p to promote self-renewal in ALDH^{High} cells.

To gain mechanistic insights into how claudin-2 regulates the phenotype of colorectal CSCs, we quantified the effect of this protein on the expression levels of microRNAs (miRNAs), which have recently emerged as dynamic regulators of self-renewal (26,27) and phenotypic plasticity (28) in CSCs.

We transfected ALDH^{High} DLD-1 cells with claudin-2-selective (siCLDN2) or control (siCON) siRNA and quantified miRNA expression 48h later using Next Generation Sequencing. A total of 1400 miRNAs were detected in ALDH^{High} DLD-1 cells. These miRNAs were analyzed for their differential expression between siCON and siCLDN2 cells (> 1.5-fold up- or down-regulation, and $p<0.05$) (Figure 6A). 468/1400 miRNA were sufficiently abundant (>20 read counts) to be reliably and reproducibly quantified, 372 of which were expressed in both siCLDN2 and siCON ALDH^{High} populations (Figure 6B). Nine miRNAs were found to be differentially expressed in siCLDN2 ALDH^{High} cells compared to controls, two down-regulated (miR-1287-5p, miR-589-3p) and seven up-regulated (miR-204-5p, miR-222-3p, miR-371b-3p, miR-372-3p, miR-373-3p, miR-629-5p, and miR-532-5p) (Figure 6C). To assess the relevance of these results in patient-derived cells, we quantified two robustly expressed miRNAs (miR-589-3p and miR-372-3p) using RT-qPCR in ALDH^{High} CPP42 cells (high endogenous claudin-2 expression) in which claudin-2 expression was down-regulated using selective siRNA transfection, and ALDH^{High} CPP1 cells (low endogenous CLDN2 expression) that were made to stably overexpress *CLDN2* (Supplemental Figure S7). Similar to what we found in DLD-1 cells, *CLDN2* down-regulation in ALDH^{High} CPP42 cells decreased miR-589-3p expression and increased miR-372-3p expression (Figure 6D). Conversely, claudin-2 overexpression in ALDH^{High} CPP1 cells increased miR-589-3p expression and decreased that of miR-372-3p (Figure 6D). These results demonstrate that claudin-2 regulates the expression of selective miRNAs in ALDH^{High} stem-like CRC cells. Interestingly, the top 10 most significantly represented molecular pathways in a KEGG pathway analysis of predicted gene targets for these 9 miRNAs included Wnt, Stem Cell and Hippo signaling (Supplemental Table S3), indicating that claudin-2 expression in ALDH^{High} cells is associated with a gene signature of CSCs and related pathways (29,30).

To determine whether the identified miRNAs play a role in the effect of claudin-2 on self-renewal, we used the DianaMicroT database to select candidate miRNAs that exhibit an enriched number of putative targets compared to what would be randomly expected within a manually curated list of 777 self-renewal-related genes (Supplemental Tables S4-S5). Three miRNAs (miR-222-3p, miR-371b-3p and miR-589-3p) were selected for further validation as described under Supplemental Methods. To determine whether preventing claudin-2-driven miRNA regulation would alter the impact of claudin-2 on self-renewal, ALDH^{high} DLD-1 cells were FACS-purified and transfected with CLDN2 siRNA in the presence or not of a miR-589-3p mimic, of miR-222-3p or miR-371b-3p inhibitors, or of their respective controls. An ELDA assay was performed to determine whether any of these treatments could block the inhibition of self-renewal observed in cells transfected with claudin-2 siRNA. We found that the miR222-3p inhibitor only was able to prevent the reduction of self-renewal induced by CLDN2 siRNAs in ALDH^{high} DLD-1 cells (Figure 6E).

CLDN2 and miRNA target gene expression were quantified to confirm treatment efficacy (Figure 6F). Expression of predicted miR-222-3p target genes such as SOX10 and cKIT was decreased in cells transfected with CLDN2-specific siRNA (Figure 6F), in agreement with the increased expression of miR-222-3p observed in these cells (Figure 6C). Expression of SOX10 and KIT returned to control levels in cells treated concomitantly with the CLDN2 siRNA and miR-222-3p inhibitor but not with CLDN2 siRNA and other miRNA inhibitors, mimics, or controls, confirming the ability of the miR-222-3p to selectively restore miR-222-3p target gene expression despite the maintained down-regulation of claudin-2 levels (Figure 6F). These findings indicate that decreased miR-222-3p expression is essential for the promotion of self-renewal by claudin-2.

Activation of YAP is necessary for claudin-2-mediated regulation of self-renewal

Because the Hippo-YAP signaling pathway is under the control of multiple protein complexes involved in cell-cell junctions and cell polarity (31), and in view of the recently identified link between miR-222 and YAP-TEAD in gastric cancer (32), we examined whether this pathway was involved in the regulation of self-renewal by claudin-2. We first examined YAP localization and quantified the expression of YAP target genes after experimental modulation of claudin-2 in CRC cells. While YAP was mostly found in the nucleus of CRC cells before or after claudin-2 down-regulation (Figure 7A) or overexpression (Figure 7B), expression of target genes (AXL, CTGF) was significantly decreased following claudin-2 down-regulation (Figure 7C) and increased in claudin-2 overexpressing cells (Figure 7B). Decrease AXL expression following claudin-2 down-regulation was only slightly reduced by the miR-589-3p mimic and miR-222-3p inhibitor (Figure 7C), suggesting that miR-222-3p, 371b-3p and 589-3p are not essential mediators of AXL regulation by claudin-2. To establish whether YAP could act upstream from miR-222-3p in mediating claudin-2-driven self-renewal, control or claudin-2-overexpressing CPP1 cells were treated with two compounds that inhibit YAP via different mechanisms, Verteporfin (33) and Simvastatin (34). miR-222-3p expression was decreased in claudin-2-overexpressing cells, and that this effect was inhibited by Verteporfin and Simvastatin treatment (Figure 7D). Treatment with these compounds also reversed the promoting effect of claudin-2 overexpression on CPP1 self-renewal (Figure 7E). Collectively these results demonstrate that increased YAP activity acts upstream from the regulation of miR-222-3p expression by claudin-2, and indicates that this pathway is instrumental for the regulation of self-renewal by claudin-2.

Discussion

In this study, we found that claudin-2 overexpression was linked with poor outcome in chemotherapy-treated stage II/III CRC patients and promoted the self-renewal properties of patient-derived CRC cells and cell lines *in vitro* and *in vitro*. High claudin-2 expression stabilized the phenotype of self-renewing CRC cells, slowing down their differentiation towards non-stem-like states and promoting the phenotypic transition of non-stem cells towards a stem-like phenotype. Claudin-2 differentially regulated the expression

of nine miRNAs in ALDH^{High} stem-like cells, and we found that activation of YAP and downstream repression of miR-222-3p were involved in the promoting effect of claudin-2 on self-renewal.

Previous studies have shown that claudin-2 expression is up-regulated during progression of CRC (6,7). However, these studies did not directly assess claudin-2 expression levels in relation with treatment and disease outcomes. Our analysis of multiple independent datasets indicates that, in patients with stage II/III CRC undergoing adjuvant chemotherapy, the high expression of CLDN2 significantly correlates with enhanced recurrence and poorer prognosis. Accordingly, the ability of claudin-2 to promote post-chemotherapy recurrence was confirmed using serial transplantation of CRC cells following chemotherapy. These findings build on recent *in vitro* studies suggesting that increased claudin-2 expression decreased the sensitivity to 5-FU (6) and are consistent with the recently reported association between claudin-2 expression and poor clinical outcome in stage IV CRC (35). In addition, claudin-2 was reported to be a negative prognostic factor and a marker of liver metastasis and early recurrence in breast cancer (36,37).

Using limiting dilution assays *in vitro* and *in vivo*, we determined that elevated claudin-2 expression in CRC cells increased the self-renewing capacity of CSCs and skewed phenotypic transitions in favor of the ALDH^{High} phenotype. This discovery of a promoting role for claudin-2 on self-renewal complements its previously reported function on the promotion of tumor growth (6) and the inhibition of cell polarity and terminal differentiation (8). We corroborated these results in several animal models of primary and metastatic tumor initiation, and our findings are thus consistent with a promoting role of claudin-2 on CSC-like cell self-renewal and with the reported role of chemo-resistant CSCs in tumor progression, metastasis initiation (20,23), and post-treatment recurrence (38). Interestingly, two other claudin isoforms (claudin-1 and/or -4) were also reported as biomarkers of progression and recurrence in oral squamous cell carcinoma (39) and lung adenocarcinoma (40), suggesting that these isoforms may also promote self-renewal in these models.

In addition, miRNA expression profiling was used to identify that claudin-2 selectively regulated the expression of several miRNAs in ALDH^{High} CSCs. miRNAs are important modulators of CSCs (41) and claudin-1 was recently shown to control miRNA dynamics in breast cancer (42). Our findings corroborate the ability of claudins to regulate miRNA expression and provide important insights into mechanisms that contribute to the control of self-renewal. Indeed, selective inhibition of miR-222-3p was found to prevent the decrease in self-renewal detected upon claudin-2 down-regulation in ALDH^{high} CRC cells, indicating that claudin-2 represses miR-222-3p in CSCs and that this contributes to its promotion of self-renewal. Interestingly, other recent reports suggested that miR-222 promotes the proliferation (43) migration and invasion (44) of CRC cells. However, these studies did not specifically analyse the 3p isoform of miR-222 and this apparent paradox may be explained by the existence of multiple naturally-existing miR-222 isoforms with distinct functions (45).

Our study also established that YAP activation was essential to the promotion of self-renewal by claudin-2 in ALDH^{high} CSCs. Key YAP target genes such as AXL and CTGF were activated by claudin-2 and

pharmacological inhibitors of this pathway reversed YAP target gene activation and prevented the claudin-2-mediated self-renewal increase. In addition, pharmacological inhibition of YAP was found to rescue the claudin-2-induced miR-222-3p repression, suggesting that YAP acts upstream from miR-222-3p in mediating the effect of claudin-2 on colorectal CSCs. Although our results do not indicate if miR-222-3p is a direct target of YAP-mediated transcription, YAP has been shown to regulate the expression of other miRNAs (46) and to regulate microRNA biogenesis in cancer cells (47).

Our findings of a role for YAP are consistent with the well-described role of YAP activity in promoting stemness and tumor initiation (48), and with the role of AXL as a key mediator of chemotherapy-induced invasion and poor clinical outcome in CRC (49). In contrast, our results may appear paradoxical in light of the described role of junction proteins in the inhibition of YAP activity in healthy and polarized epithelia (31). However, in polarized tissues cell junction proteins form highly-organized membrane complexes and usually drive contact inhibition by activating Hippo signalling and sequestering YAP away from the nucleus, thereby blocking its transcriptional activity (31). In the context of colorectal tumor cells, where polarity and contact inhibition are at least partially lost, our results indicate that overexpression of claudin-2 enhances the YAP activity without strongly affecting its nuclear localization, supporting the observation by others that regulation of YAP in tumor cells can be independent from Hippo (48).

In conclusion, our findings indicate that high expression of claudin-2 in colorectal tumors promotes CSC self-renewal and hampers their transition towards more differentiated phenotypes. This provides a credible rationale for the potential development of claudin-2 selective antibodies as prospective tools to decrease the self-renewal potential of colorectal CSCs. A proof of concept for therapeutic usage of claudin-specific antibodies has recently been established, with the claudin-18.2 antibody IMAB362 currently undergoing phase II clinical trials in gastrointestinal, esophageal and ovarian cancer (NCT01630083, NCT020054351 and NCT01197885 at www.clinicaltrials.gov). From a mechanistic perspective, our findings unravel a novel mechanism implicating the claudin-2/YAP/miR-222-3p axis and linking the cell membrane to the regulation of self-renewal in CRC cells.

Acknowledgements: the authors wish to thank Drs Hyun-Jung Cho and Paul McMillan (BOMP imaging facility, University of Melbourne) and Dr Vanta Jameson (Flow Cytometry facility, University of Melbourne) for their technical support. They are also very grateful to Prof. K. Harvey for helpful discussions and for sharing Hippo/YAP pathway reagents. Biospecimens and data used for TMA immunostaining experiments were obtained from the Victorian Cancer Biobank, Victoria, Australia with appropriate ethics approval. The Victorian Cancer Biobank is supported by the Victorian Government.

References

1. Lal-Nag M, Morin PJ. The claudins. Genome biology 2009;10(8):235.

2. Gupta IR, Ryan AK. Claudins: unlocking the code to tight junction function during embryogenesis and in disease. Clinical genetics 2010;77(4):314-25.

3. Morin PJ. Claudin proteins in human cancer: promising new targets for diagnosis and therapy. Cancer research 2005;65(21):9603-6.

4. Darido C, Buchert M, Pannequin J, Bastide P, Zalzali H, Mantamadiotis T, et al. Defective claudin-7 regulation by Tcf-4 and Sox-9 disrupts the polarity and increases the tumorigenicity of colorectal cancer cells. Cancer research 2008;68(11):4258-68.

5. Singh AB, Sharma A, Smith JJ, Krishnan M, Chen X, Eschrich S, et al. Claudin-1 up-regulates the repressor ZEB-1 to inhibit E-cadherin expression in colon cancer cells. Gastroenterology 2011;141(6):2140-53.

6. Dhawan P, Ahmad R, Chaturvedi R, Smith JJ, Midha R, Mittal MK, et al. Claudin-2 expression increases tumorigenicity of colon cancer cells: role of epidermal growth factor receptor activation. Oncogene 2011;30(29):3234-47.

7. Kinugasa T, Huo Q, Higashi D, Shibaguchi H, Kuroki M, Tanaka T, et al. Selective up-regulation of claudin-1 and claudin-2 in colorectal cancer. Anticancer research 2007;27(6A):3729-34.

8. Buchert M, Papin M, Bonnans C, Darido C, Raye WS, Garambois V, et al. Symplekin promotes tumorigenicity by up-regulating claudin-2 expression. Proceedings of the National Academy of Sciences of the United States of America 2010;107(6):2628-33.

9. Rahner C, Mitic LL, Anderson JM. Heterogeneity in expression and subcellular localization of claudins 2, 3, 4, and 5 in the rat liver, pancreas, and gut. Gastroenterology 2001;120(2):411-22.

10. Ahmad R, Chaturvedi R, Olivares-Villagomez D, Habib T, Asim M, Shivesh P, et al. Targeted colonic claudin-2 expression renders resistance to epithelial injury, induces immune suppression, and protects from colitis. Mucosal immunology 2014;7(6):1340-53.

11. Bonnans C, Flaceliere M, Grillet F, Dantec C, Desvignes JP, Pannequin J, et al. Essential requirement for beta-arrestin2 in mouse intestinal tumors with elevated Wnt signaling. Proceedings of the National Academy of Sciences of the United States of America 2012;109(8):3047-52.

12. Adorno-Cruz V, Kibria G, Liu X, Doherty M, Junk DJ, Guan D, et al. Cancer stem cells: targeting the roots of cancer, seeds of metastasis, and sources of therapy resistance. Cancer research 2015;75(6):924-9.

13. Planque C, Rajabi F, Grillet F, Finetti P, Bertucci F, Gironella M, et al. Pregnane X-receptor promotes stem cell-mediated colon cancer relapse. Oncotarget 2016;7(35):56558-73.

14. Giraldez MD, Lozano JJ, Cuatrecasas M, Alonso-Espinaco V, Maurel J, Marmol M, et al. Gene-expression signature of tumor recurrence in patients with stage II and III colon cancer treated with 5'fluoruracil-based adjuvant chemotherapy. International journal of cancer 2013;132(5):1090-7.

15. Sveen A, Agesen TH, Nesbakken A, Rognum TO, Lothe RA, Skotheim RI. Transcriptome instability in colorectal cancer identified by exon microarray analyses: Associations with splicing factor expression levels and patient survival. Genome medicine 2011;3(5):32.

16. Aguirre-Gamboa R, Gomez-Rueda H, Martinez-Ledesma E, Martinez-Torteya A, Chacolla-Huaringa R, Rodriguez-Barrientos A, et al. SurvExpress: an online biomarker validation tool and database for cancer gene expression data using survival analysis. PloS one 2013;8(9):e74250.

17. Marisa L, de Reynies A, Duval A, Selves J, Gaub MP, Vescovo L, et al. Gene expression classification of colon cancer into molecular subtypes: characterization, validation, and prognostic value. PLoS medicine 2013;10(5):e1001453.

18. Giraud J, Failla LM, Pascussi JM, Lagerqvist EL, Ollier J, Finetti P, et al. Autocrine Secretion of Progastrin Promotes the Survival and Self-Renewal of Colon Cancer Stem-like Cells. Cancer research 2016;76(12):3618-28.

19. Dawood S, Austin L, Cristofanilli M. Cancer stem cells: implications for cancer therapy. Oncology (Williston Park, NY) 2014;28(12):1101-7, 10.

20. Todaro M, Francipane MG, Medema JP, Stassi G. Colon cancer stem cells: promise of targeted therapy. Gastroenterology 2010;138(6):2151-62.

21. Islam F, Gopalan V, Smith RA, Lam AK. Translational potential of cancer stem cells: A review of the detection of cancer stem cells and their roles in cancer recurrence and cancer treatment. Experimental cell research 2015;335(1):135-47.

22. Kreso A, O'Brien CA. Colon cancer stem cells. Current protocols in stem cell biology 2008;Chapter 3:Unit 3.1.

23. Kreso A, Dick JE. Evolution of the cancer stem cell model. Cell stem cell 2014;14(3):275-91.

24. Huang EH, Hynes MJ, Zhang T, Ginestier C, Dontu G, Appelman H, et al. Aldehyde dehydrogenase 1 is a marker for normal and malignant human colonic stem cells (SC) and tracks SC overpopulation during colon tumorigenesis. Cancer research 2009;69(8):3382-9.

25. Gupta PB, Fillmore CM, Jiang G, Shapira SD, Tao K, Kuperwasser C, et al. Stochastic state transitions give rise to phenotypic equilibrium in populations of cancer cells. Cell 2011;146(4):633-44.

26. Deng L, Shang L, Bai S, Chen J, He X, Martin-Trevino R, et al. MicroRNA100 inhibits self-renewal of breast cancer stem-like cells and breast tumor development. Cancer research 2014;74(22):6648-60.

27. Wang H, Sun T, Hu J, Zhang R, Rao Y, Wang S, et al. miR-33a promotes glioma-initiating cell self-renewal via PKA and NOTCH pathways. The Journal of clinical investigation 2014;124(10):4489-502.

28. Zhu Y, Luo M, Brooks M, Clouthier SG, Wicha MS. Biological and clinical significance of cancer stem cell plasticity. Clinical and translational medicine 2014;3(1):32.

29. Hao J, Zhang Y, Jing D, Li Y, Li J, Zhao Z. Role of Hippo signaling in cancer stem cells. Journal of cellular physiology 2014;229(3):266-70.

30. Reya T, Clevers H. Wnt signalling in stem cells and cancer. Nature 2005;434(7035):843-50.

31. Gumbiner BM, Kim NG. The Hippo-YAP signaling pathway and contact inhibition of growth. Journal of cell science 2014;127(Pt 4):709-17.

32. Li N, Yu N, Wang J, Xi H, Lu W, Xu H, et al. miR-222/VGLL4/YAP-TEAD1 regulatory loop promotes proliferation and invasion of gastric cancer cells. American journal of cancer research 2015;5(3):1158-68.

33. Brodowska K, Al-Moujahed A, Marmalidou A, Meyer Zu Horste M, Cichy J, Miller JW, et al. The clinically used photosensitizer Verteporfin (VP) inhibits YAP-TEAD and human retinoblastoma cell growth in vitro without light activation. Experimental eye research 2014;124:67-73.

34. Wang Z, Wu Y, Wang H, Zhang Y, Mei L, Fang X, et al. Interplay of mevalonate and Hippo pathways regulates RHAMM transcription via YAP to modulate breast cancer cell motility. Proceedings of the National Academy of Sciences of the United States of America 2014;111(1):E89-98.

35. Mezheyeuski A, Strell C, Hrynchyk I, Guren TK, Dragomir A, Doroshenko T, et al. Treatment-related survival associations of claudin-2 expression in fibroblasts of colorectal cancer. Virchows Archiv : an international journal of pathology 2017.

36. Kimbung S, Kovacs A, Bendahl PO, Malmstrom P, Ferno M, Hatschek T, et al. Claudin-2 is an independent negative prognostic factor in breast cancer and specifically predicts early liver recurrences. Molecular oncology 2014;8(1):119-28.

37. Tabaries S, Dupuy F, Dong Z, Monast A, Annis MG, Spicer J, et al. Claudin-2 promotes breast cancer liver metastasis by facilitating tumor cell interactions with hepatocytes. Molecular and cellular biology 2012;32(15):2979-91.

38. Colak S, Medema JP. Cancer stem cells--important players in tumor therapy resistance. The FEBS journal 2014;281(21):4779-91.

39. DE Vicente J, Fernandez-Valle A, Vivanco-Allende B, Santamarta TR, Lequerica-Fernandez P, Hernandez-Vallejo G, et al. The prognostic role of claudins -1 and -4 in oral squamous cell carcinoma. Anticancer research 2015;35(5):2949-59.

40. Chae MC, Park CK, Keum DY, Hwang I, Kwon KY, Jang BC. Prognostic significance of claudin 4 in completely resected adenocarcinoma of the lung. The Korean journal of thoracic and cardiovascular surgery 2014;47(3):262-8.

41. Garofalo M, Croce CM. Role of microRNAs in maintaining cancer stem cells. Advanced drug delivery reviews 2015;81:53-61.

42. Majer A, Blanchard AA, Medina S, Booth SA, Myal Y. Claudin 1 Expression Levels Affect miRNA Dynamics in Human Basal-Like Breast Cancer Cells. DNA and cell biology 2016;35(7):328-39.

43. Liu S, Sun X, Wang M, Hou Y, Zhan Y, Jiang Y, et al. A microRNA 221- and 222-mediated feedback loop maintains constitutive activation of NFkappaB and STAT3 in colorectal cancer cells. Gastroenterology 2014;147(4):847-59.e11.

44. Gao H, Cong X, Zhou J, Guan M. MicroRNA-222 influences migration and invasion through MIA3 in colorectal cancer. Cancer cell international 2017;17:78.

45. Yu F, Pillman KA, Neilsen CT, Toubia J, Lawrence DM, Tsykin A, et al. Naturally existing isoforms of miR-222 have distinct functions. Nucleic acids research 2017;45(19):11371-85.

46. Shen S, Guo X, Yan H, Lu Y, Ji X, Li L, et al. A miR-130a-YAP positive feedback loop promotes organ size and tumorigenesis. Cell research 2015;25(9):997-1012.

47. Yu FX, Guan KL. Transcription and processing: multilayer controls of RNA biogenesis by the Hippo pathway. The EMBO journal 2014;33(9):942-4.

48. Zanconato F, Cordenonsi M, Piccolo S. YAP/TAZ at the Roots of Cancer. Cancer Cell 2016;29(6):783-803.

49. Dunne PD, McArt DG, Blayney JK, Kalimutho M, Greer S, Wang T, et al. AXL is a key regulator of inherent and chemotherapy-induced invasion and predicts a poor clinical outcome in early-stage colon cancer. Clinical cancer research : an official journal of the American Association for Cancer Research 2014;20(1):164-75.

Figure Legends

Figure 1: Higher levels of CLDN2 are associated with post-treatment recurrence in stage II and III CRC patients

Kaplan-Meier curves reflecting the difference of cancer-specific (A) and recurrence-free survival (B, C) among chemotherapy-treated stage II and III CRC patient in relation with the claudin-2 mRNA expression levels (*CLDN2*) in their primary tumor sample. **A.** Cancer-specific survival rate in a cohort of 86 patients, high *CLDN2*-expressing (red line) vs low *CLDN2*-expressing group (blue line). **B.** Recurrence free survival in 461 patients (GSE39582 dataset), analyzed using the R2 Genomics Analysis and Visualisation Platform (http://r2.amc.nl). High *CLDN2*-expressing group (red line), low CLDN2-expressing group (blue line). **C.** Recurrence free survival in 160 patients indicated (GSE24551), analyzed using the SurvExpress bioresource (http://bioinformatica.mty.itesm.mx:8080/Biomatec/SurvivaX.jsp). High *CLDN2*-expressing group (red line), low *CLDN2*-expressing group (blue line). **D.** *CLDN2* gene expression level in Low and High Risk patients (data as in C). **E.** Claudin-2 immunostaining in tumor tissue sections from stage II/III CRC patients. Images are representative of the observed staining pattern intensities (Negative to Strong) and subcellular distributions (Membrane and/or Diffuse).

Figure 2: Claudin-2 promotes self-renewal of CRC cells

Experimental modification of claudin-2 expression levels regulates self-renewal in several CRC cell lines. In B, D and E, results are expressed as mean ± SEM, n = 3 (Student t-test, ** $p<0.01$).

A. Top panel, Claudin-2 expression in SW480 CRC cells was quantified by Western Blot in cells expressing a tetracycline-inducible claudin-2 (CLDN2) or control construct (CON), treated or not with doxycycline (DOX) for 24h, 48h and 96h. Levels of β-actin expression are used as internal loading controls. Bottom panel, immunofluorescence detection of claudin-2 at the plasma membrane of cells expressing the claudin-2 construct (CLDN2), while claudin-2 expression is barely detectable in control cells (CON). Nuclei are counter stained with DAPI, scale bars=50 µm. **B.** Colonosphere formation was quantified in SW480 cells over-expressing Claudin-2 (CLDN2) or expressing a control vector (CON), at passage one (P1, top panel) or after four passages (P4, bottom panels). The number of colonospheres formed was quantified. **C.** Extreme limiting dilution analysis (ELDA) was used to determine the self-renewal frequency of CPP1 patient-derived cells. The presence or absence of spheres was assessed seven days after seeding at 1000, 100 or 10 or 1 cells/well (each concentration in 12 replicates) in an ultra-low adherence 96-well plate, and reported as the estimated sphere-forming frequency + confidence intervals ($p = 0.0219$, Chi-square, n = 3). **D.** Quantification of claudin-2 expression by Western blotting (top left) and immunofluorescent staining (bottom left, nuclei counterstained with DAPI) in DLD-1 cells expressing a claudin-2-specific shRNA (shCLDN2) or a control shRNA (shCON) (scale bars= 50 µm). Right panel, colonosphere formation was quantified in shCON and shCLDN2 DLD-1 cells. **E.** Colonosphere formation was quantified in T84 cells

expressing a claudin-2-specific shRNA (shCLDN2) or a control shRNA (shCON) after one (P1) or two passages (P2) in suspension. show that colonospheres are decreased when *CLDN2* expression is downregulated. Analysis as mentioned in B. **F.** Three-dimensional CRC patient-derived colon organoids. Patient tumor cells from the colon were isolated, transfected with siRNA against CLDN2, and grown in Matrigel. Phase-contrast photographs (left) exemplify the development of three-dimensional organoids at day 3. The initiation of organoids (diameter ≥ 30μm) was decreased after claudin-2-specific siRNA transfection (siCLDN2, 50 mM), in comparison with controls (siCON) (scale bars = 50 μm). The mean incidence of organoids after three days is shown on the right panel (non-transfected controls = NT) (siCON vs siCLDN2 p = 0.0426, ANOVA with Tukey's multiple comparisons test, n = 6).

Figure 3: Claudin-2 promotes CRC tumor initiation and self-renewal *in vivo*

Tumor incidence was quantified after subcutaneous xenografting of CRC cell lines stably overexpressing claudin-2 (CLDN2) or vector control cells (CON) into first and second generation NOD/SCID mice (n = 5 per group). **A.** Left panel, first-generation xenografts generated with patient-derived CPP1 cells at 50 or 500 or 5000 cells/injection. Right panel, tumors collected from first generation mice injected with 500 cells were harvested, pooled and serially re-injected to second generation animals, followed by regular monitoring of tumor intake and size. ‡ signifies that all mice were euthanized. **B.** Left panel, tumor incidence was quantified following inoculation of 10 or 100 or 1000 CMT93 cells expressing a control or claudin-2 expressing construct. Right panel, representative photographs of tissue sections obtained from control or claudin-2 overexpressing xenografts and immunostained with a specific claudin-2 antibody. Photographs from two representative control tumors (CON) and two claudin-2 overexpressing tumors (CLDN2) (1000 cells/injection) harvested at D37 are shown (scale bar=100 μm). **C.** Top panel, outline of chemotherapy and post-treatment re-implantation protocol of T84 cell xenografts. Bottom, claudin-2 expression in post-treatment tumor cells prior to re-implantation into second generation animals (left, * Student t-test, $p < 0.05$), and tumor incidence in second generation animals injected with decreasing amounts of control or claudin-2 shRNA-expressing T84 cells (right).

Figure 4: Claudin-2 promotes the CSC phenotype *in vitro*

A. Expression of the mRNAs for *CLDN2*, *BMI1* and *Oct-4* in T84 cells stably transfected with control of claudin-2 specific shRNAs (Student's t test, * $p < 0.01$, mean ± SEM, n = 3). **B.** Expression of the mRNAs for *CLDN2*, *BMI1*, *ALDH1A1*, and *Oct-4* in DLD-1 (left panel), T84 (middle panel) and patient-derived CPP42 cells (right panel) 24h after transient transfection with siRNA targeting CLDN2, expressed as fold-change compared to their respective expression in cells expressing a β-galactosidase-specific control siRNA (mean ± SEM from experimental replicates, data from one of two similar experiments, Student t-test, * $p < 0.05$, ** $p < 0.01$,** * $p < 0.001$). **C.** *CLDN2* mRNA expression in $ALDH^{Low}$ and $ALDH^{High}$ T84 cells (mean ± SEM). **D.** Percentages of $ALDH^{Low}$ (grey) and $ALDH^{High}$ cells (white) in untransfected T84 cells

(top), as well as 3 days after transfection with siRNA selectively targeting CLDN2 (siCLDN2) or β-galactosidase (siCON) (Data representing one of three similar experiments). **E.** Purified T84 $ALDH^{High}$ cells (white, top) or $ALDH^{Low}$ cells (grey, bottom) were independently transfected with a β-galactosidase-specific control siRNA (siCON) or with a claudin-2 specific siRNA (siCLDN2), and the percentages of $ALDH^{High}$ and $ALDH^{Low}$ cells were re-analyzed in each population 3 days and 6 days after transfection (Data represents one of three similar experiments).

Figure 5: Claudin-2 promotes CSCs self-renewal *in vitro* and tumorigenic capacities *in vivo*

A. Extreme limiting dilution analysis was used to determine the self-renewal frequency of $ALDH^{High}$ T84 cells transiently transfected with a claudin-2- (siCLDN2) or a β-galactosidase-specific (siCON) siRNA. The presence or absence of spheres was quantified seven days after seeding at 1000, 100 or 10 or 1 cells/well (each concentration in 12 replicates) in an ultra-low adherence 96-well plate, and reported as the estimated sphere-forming frequency + confidence intervals ($p = 0.000132$, Chi-square, representative replicate from 3 experiments). **B.** Tumor incidence measured 4 to 7 weeks after inoculation of NOD/SCID mice with purified $ALDH^{High}$ T84 cells transfected with siCLDN2 or siCON as described under supplemental Methods, (500 cells /injection, n = 5 per group). **C.** Representative macroscopic appearance of T84 xenografts induced after subcutaneous inoculation of control siRNA transfected (siCON) or siCLDN2 transfected (siCLDN2) $ALDH^{High}$ T84 cells, and harvested after 7 weeks. Black dotted circle shows lack of tumor initiation at the inoculation site. **D.** Scatter plot showing the expression level of *CLDN2* mRNA in 10 patient-derived CRC cell populations, separated into two subgroups based on their stem cell frequencies (Low or High, x axis) (mean ± SEM, unpaired t-test, two-tailed, * $p<0.05$).

Figure 6: miR-222-3p is involved in claudin-2-mediated regulation of self-renewal in $ALDH^{High}$ cells

A. Volcano plot summarizing the differential expression of miRNAs (fold-change (x-axis) and p-value (y-axis)) in $ALDH^{High}$ DLD-1 cells transfected with a claudin-2- (siCLDN2) or a β-galactosidase-specific (siCON) siRNA. Each dot represents one miRNA (red= significantly up-regulated, green = significantly down-regulated, grey= no significant differential expression; blue lines= threshold of significance). **B.** Venn diagram showing the number of miRNAs detected in siCLDN2 (n = 64), siCON (n = 32), or both siCLDN2 and siCON (n = 372) $ALDH^{High}$ DLD-1 cells ($p<0.05$, n = 3). **C.** Heat map representing differential expression of 9 miRNAs ($p<0.05$, ± 1.5 Fold change, > 20 read counts) in $ALDH^{High}$ DLD-1 cells transfected with a claudin-2- (siCLDN2) or a β-galactosidase-specific (siCON) siRNA. **D.** qRT-PCR expression levels for miR-589-3p and miR-372-3p in CPP42cells (expressing siCLDN2 or siCON) and in CPP1 cells (overexpressing CLDN2 (CLDN2+) or a control vector (CON)). Data from one representative experiment is shown (n = 2). **E.** Sphere-forming frequency of $ALDH^{High}$ DLD-1 cells transfected with β-galactosidase or claudin-2-specific siRNA with or without mimics or inhibitors for miR-222-3p, 371b-3p or

589-3p as indicated, as determined using an Extreme Limiting Dilution Analysis after seeding at 1000, 100, 30, 10 and 3 cells/well in ultra-low adherence plates (each concentration in 10-12 replicates) (n = 3). Scoring was performed 9-11 days after transfection and data is reported as the estimated sphere-forming frequency + confidence intervals, as well as estimated percentage of self-renewing cells. Statistical analysis of differences between groups was performed using the Chi-square test. **F.** Expression of mRNAs encoding Claudin-2 as well as miRNA target genes (predicted using Diana MicroT) was quantified using RT-qPCR 24h after transfection of $ALDH^{High}$ DLD-1 cells with β-galactosidase or claudin-2-specific siRNA with or without mimics or inhibitors for miR-222-3p, 371b-3p or 589-3p. Data is expressed as fold-change compared to β-galactosidase siRNA-transfected cells (n = 3, * $p < 0.05$ compared to siBgal, # $p < 0.05$ compared to siCLDN2 + control inhibitor, two-way ANOVA + Tukey multiple comparison test).

Figure 7: YAP acts upstream from miR-222-3p to mediate claudin-2-promoted self-renewal

A. Immunofluorescent staining of claudin-2 and YAP in DLD-1 CRC cells transfected with β-galactosidase (control) or claudin-2 specific siRNA. Nuclei are stained using DAPI. Bars = 50μm. **B.** Decreased mRNA expression for the key YAP target gene AXL in $ALDH^{high}$ DLD-1 cells transfected with β-galactosidase or claudin-2-specific siRNA with or without mimics or inhibitors for miR-222-3p, 371b-3p or 589-3p as indicated, as quantified using RT-qPCR. $p < 0.05$ compared to siBgal (*) or to siCLDN2 (#), ANOVA with Tukey post-hoc test. **C.** YAP immunostaining and expression of YAP target genes in CPP1 patient-derived cells expressing a control or claudin-2-encoding vector. *, $p < 0.05$ compared to control CPP1 cells, Student t-test. Expression of claudin-2 in these cells is shown in Suppl. Figure S2. **D.** Expression of miR-222-3p in control or claudin-2 expressing CPP1 cells treated with vehicle, Verteporfin or Simvastatin as indicated, quantified using the Taqman microRNA assays. Data from a representative experiment is expressed as fold-change compared to vehicle-treated control CPP1 cells (n = 3 technical replicates). **E.** Sphere-forming frequency in control (CT) or claudin-2 expressing CPP1 cells, determined using an Extreme Limiting Dilution Analysis after seeding at 1000, 100, 10 and 1 cells/well in ultra-low adherence plates (each concentration in 12 replicates) and treating with vehicle, Verteporfin or Simvastatin as indicated. Scoring was performed 7-9 days after seeding and data is reported as the estimated sphere-forming frequency + confidence intervals, as well as estimated percentage of self-renewing cells. Statistical analysis of differences between groups was performed using the Chi-square test.

Figure 1

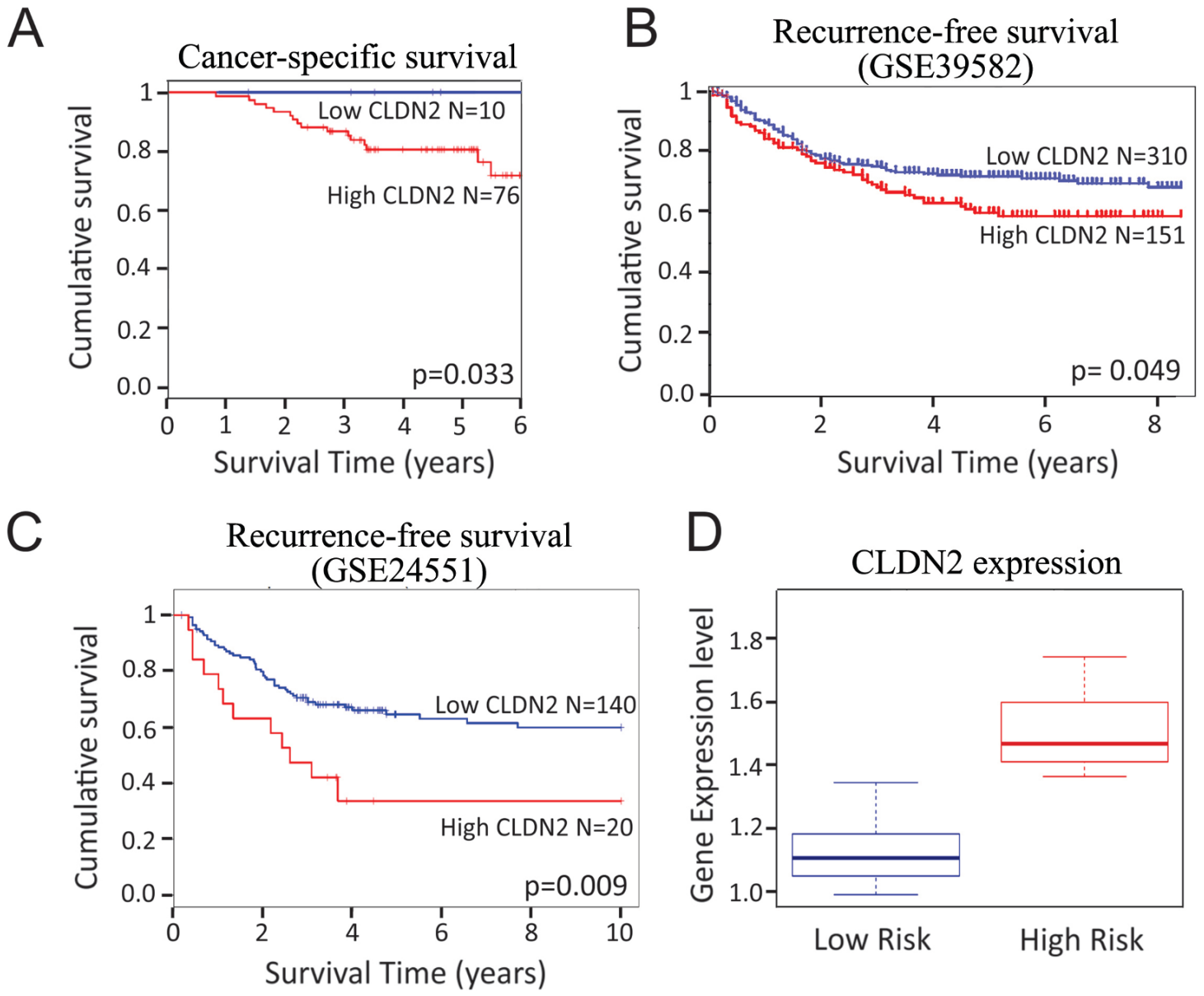

Figure 2

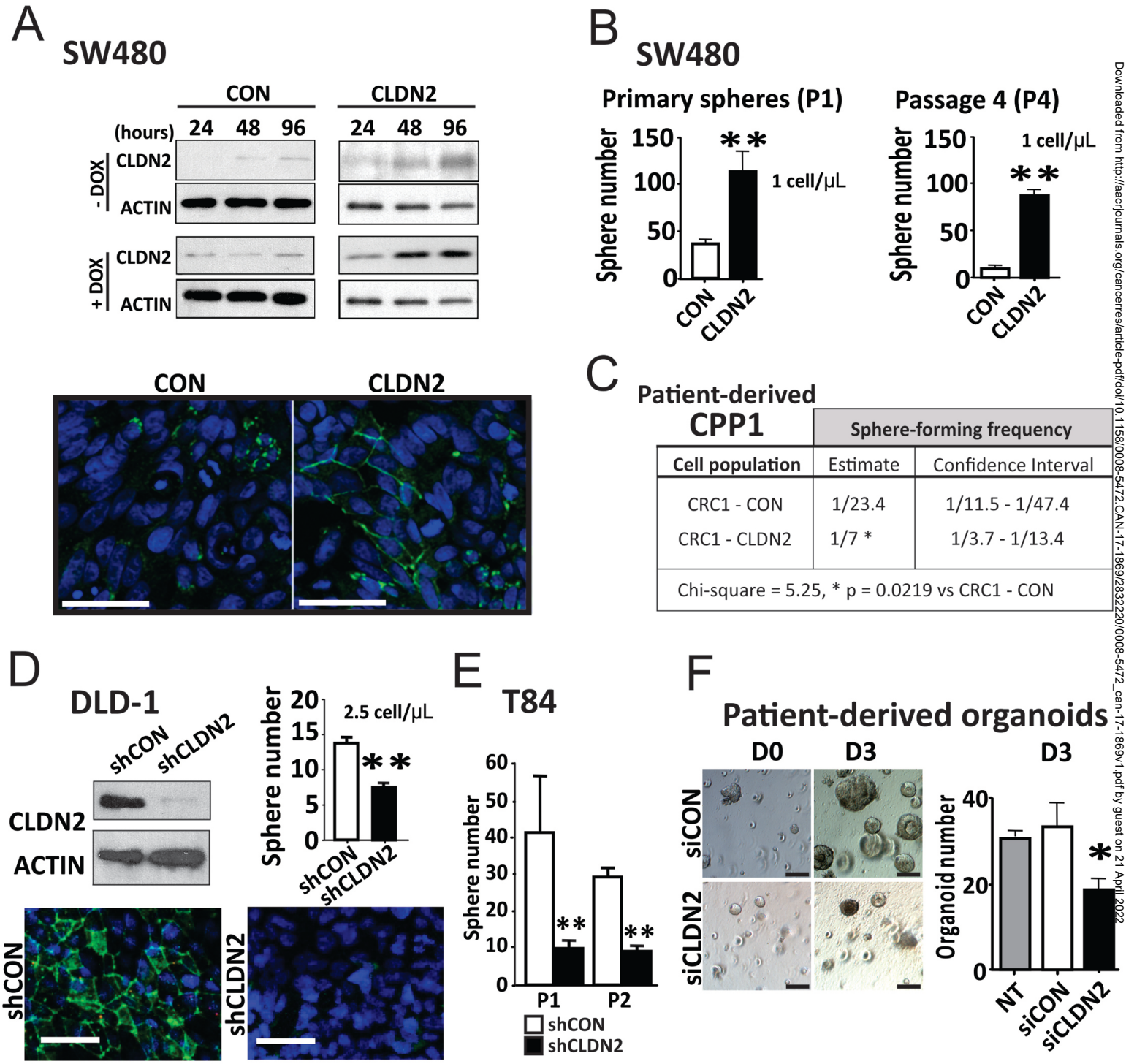

Figure 3

A

Patient-derived CPP1

Sub-cutaneous (sc.) inoculation #1 → Tumors pooled & reimplanted → sc. inoculation #2

Tumor incidence	D14	D47	D62	D71	D90
CLDN2 50c	0/5	0/5	0/5	0/5	3/5
CLDN2 500c	0/5	5/5	5/5	‡	‡
CLDN2 5000c	1/5	5/5	5/5	5/5	‡
CON 50c	0/5	0/5	0/5	0/5	0/5
CON 500c	0/5	0/5	4/5	5/5	‡
CON 5000c	0/5	0/5	3/5	5/5	‡

Tumor incidence	D35	D70
CLDN2 50c	1/5	1/5
CLDN2 500c	2/5	4/5
CLDN2 5000c	3/5	4/5
CON 50c	N/A	
CON 500c		
CON 5000c		

B

CMT93

Tumor incidence	D21	D37
CLDN2 10c	0/5	1/5
CLDN2 100c	0/5	5/5
CLDN2 1000c	5/5	5/5
CON 10c	0/5	0/5
CON 100c	0/5	0/5
CON 1000c	0/5	4/5

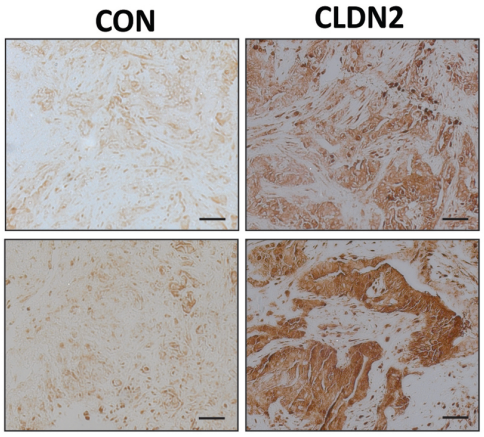

C

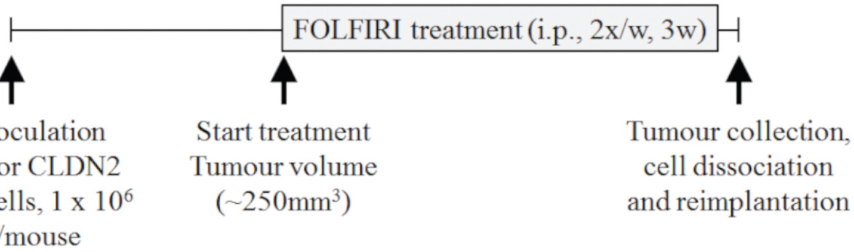

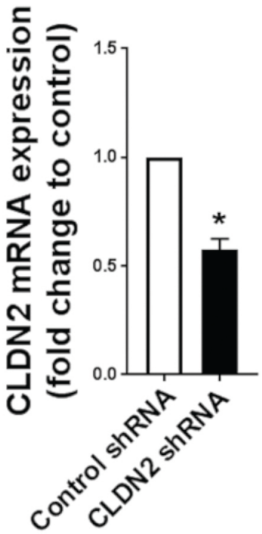

	Reimplantation dose and tumor incidence		
T84 cells	5000 cells	500 cells	50 cells
Control shRNA	6/6	4/6	5/6
CLDN2 shRNA	2/6	3/6	2/6

Figure 4

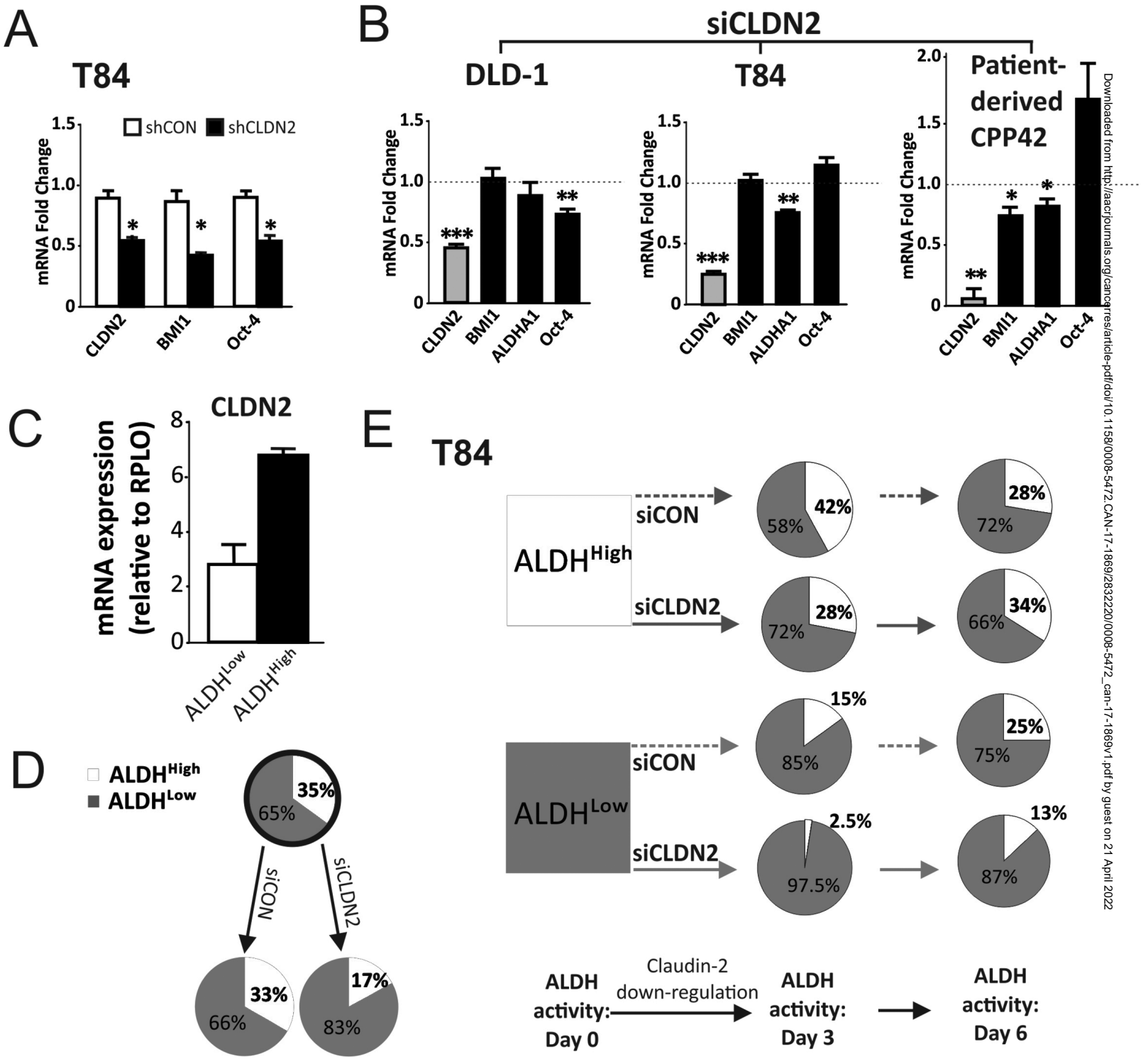

Figure 5

A

T84

Cell population	Sphere-forming frequency	
	Estimate	Confidence Interval
T84 siCON	1/6.24	1/3.31 - 1/11.8
T84 siCLDN2	1/39.8*	1/21.2- 1/74.8

Chi-square = 14.6, * p = 0.000132 vs T84 siCON

B

Tumour incidence	4w	5w	6w	7w
siCON	0/5	5/5	5/5	5/5
siCLDN2	0/5	1/5	2/5	2/5

C

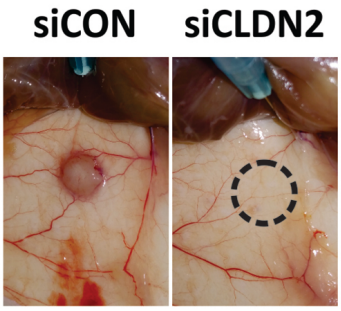

D

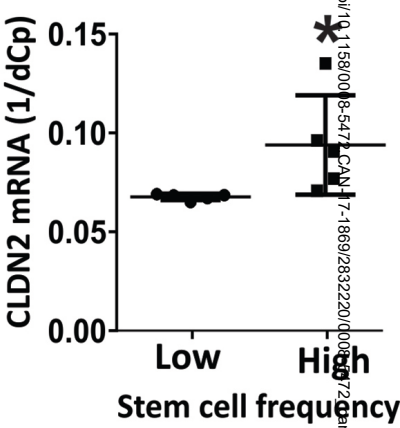

Figure 6

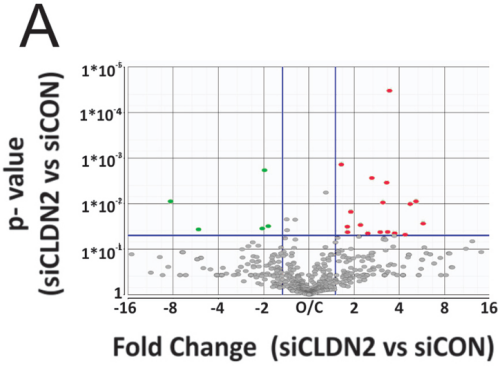

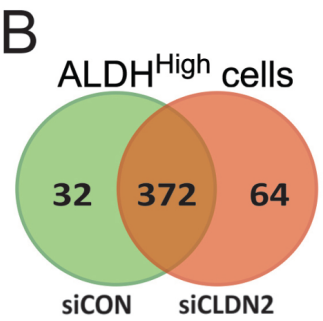

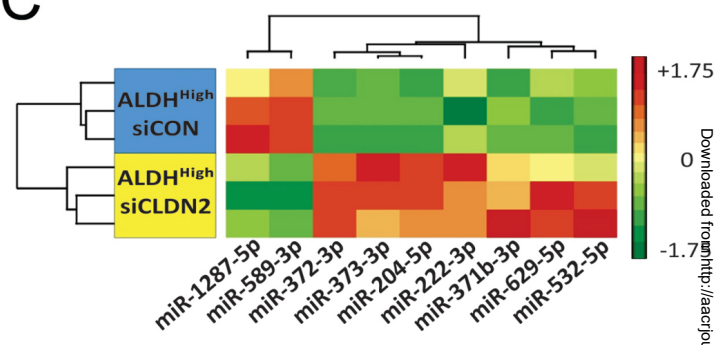

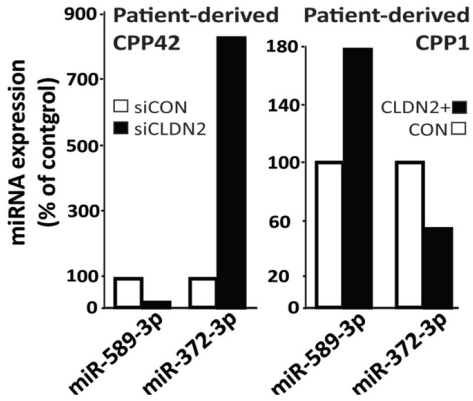

E

ALDH^High DLD1 cells	Sphere-forming frequency	
Treatment condition	**Estimate (confidence interval)**	**%**
siBgal	1/7.68 (1/10.76 - 1/5.52)	13.02
siCLDN2	16.96 (1/23.77 - 1/12.14) *(*)*	5.90
siCLDN2 + CT mimic	1/20.05 (1/28.12 - 1/14.33) *(†)*	4.99
siCLDN2 + miR-589-3p mimic	1/24.73 (1/34.66 - 1/17.68) *(†)*	4.04
siCLDN2 + CT inhibitor	1/16.42 (1/23.01 - 1/11.76) *(†)*	6.09
siCLDN2 + miR-222-3p inhibitor	1/6.35 (1/8.93 - 1/4.57) *(#)(††)*	15.75
siCLDN2 + miR-371b-3p inhibitor	1/14.75 (1/20.65 - 1/10.58) *(†)*	6.78

* Chi-square = 9.71, p = 0.0018; siBgal vs siCLDN2

\# Chi-square = 7.39, p = 0.0065; siCLDN2 vs siCLDN2 + miR-222-3p inhibitor

Chi-square = 10.8, p = 0.0010; siCLDN2 vs siCLDN2 + mi-R371b-3p inhibitor

† p > 0.05 vs siCLDN2

†† p > 0.05 vs siBgal

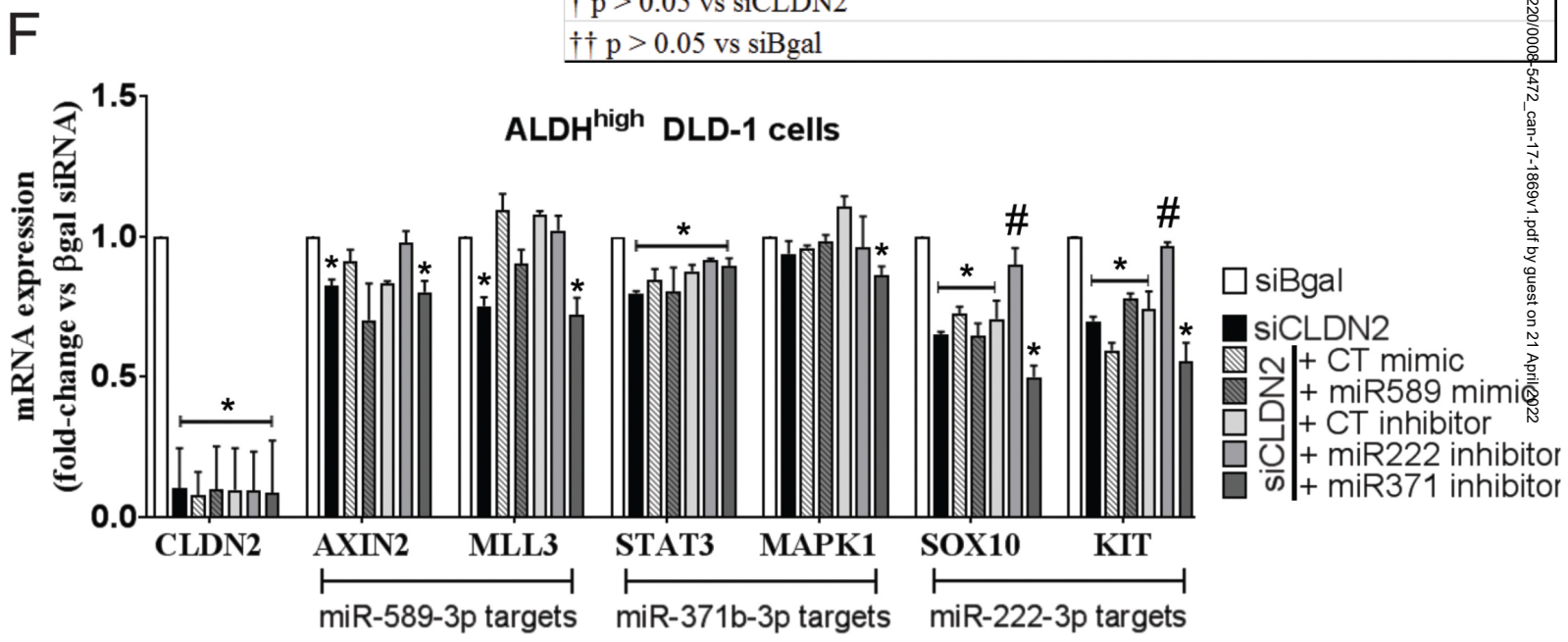

Figure 7

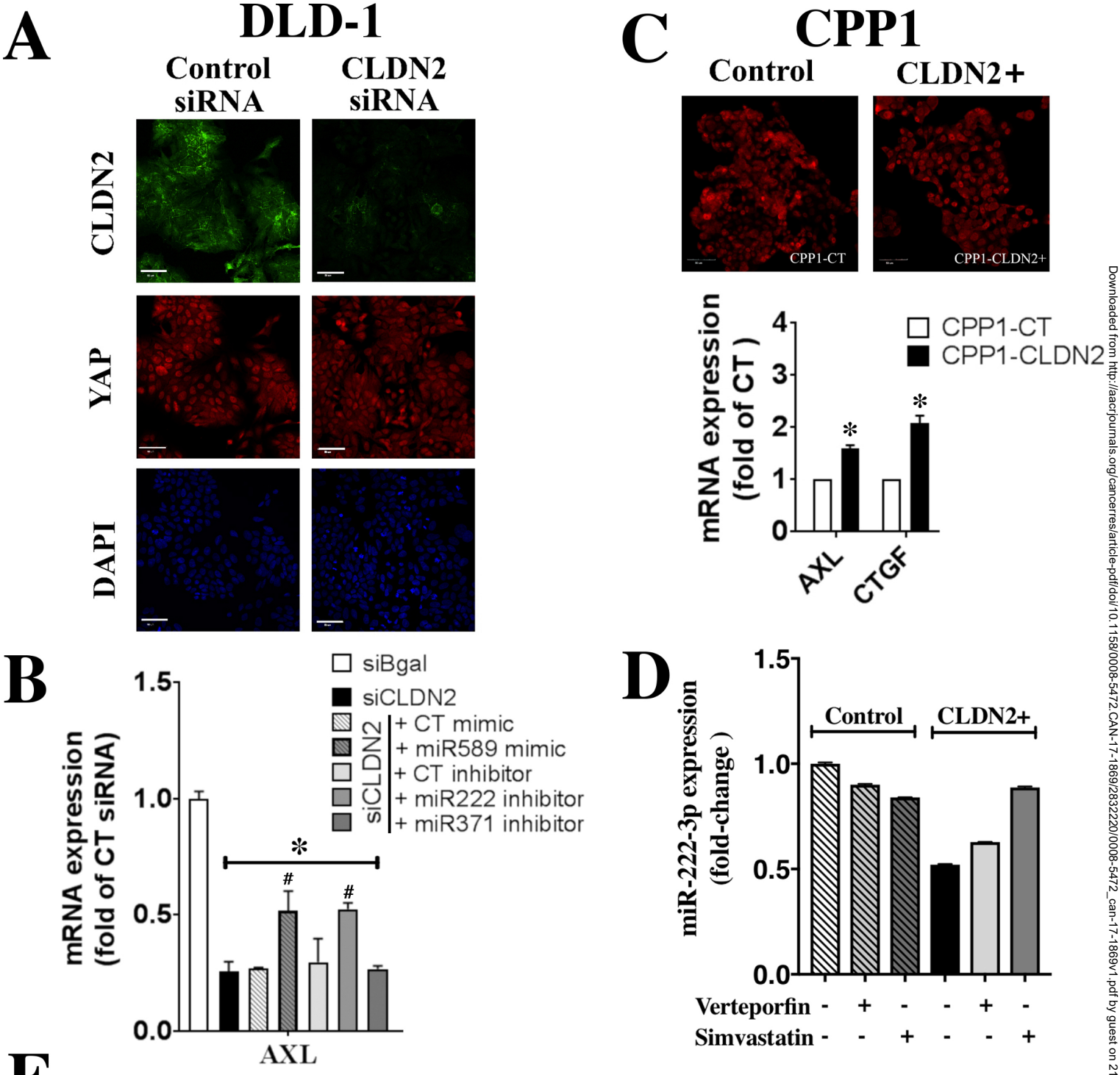

E

CPP1 cells	Sphere-forming frequency	
Treatment condition	**Estimate (confidence interval)**	**%**
CT + vehicle	1/22.39 (1/36.8-1/13.7)	4.47
CT + Simvastatin 4 microM	1/57.72 (1/107.3 - 1/31.15)*	1.73
CT + VP 0.5microg/ml	1/20.04 (1/41.1 - 1/9.91)	4.99
CLDN2 + vehicle	1/9.64 (1/15.2 - 1/6.19)*	10.37
CLDN2 + Simvastatin 4 microM	1/32.81 (1/62.6 - 1/17.3)#	3.05
CLDN2 + VP 0.5microg/ml	1/20.57 (1/42.1 - 1/10.2)	4.86
* Chi-square > 5.50, p < 0.002 vs CT + vehicle		
# Chi-square = 8.25, p = 0.004; CLDN2 + Simvastatin vs CLDN2 + vehicle		
† Chi-square = 4.2, p = 0.0405; CLDN2 + VP vs CLDN2 + vehicle		